Published in final edited form as:
Exp Eye Res. 2014 January ; 118: 61–71. doi:10.1016/j.exer.2013.10.009.

In vitro moxifloxacin drug interaction with chemotherapeutics: implications for retinoblastoma management

Megha Barot, **Mitan R. Gokulgandhi**, **Dhananjay Pal**, and **Ashim K. Mitra***
Division of Pharmaceutical Sciences, School of Pharmacy, University of Missouri-Kansas City, 2464 Charlotte Street, Kansas City, MO 64108, USA.

Abstract

Retinoblastoma (RB) is a common malignant intraocular tumor primarily affecting children. Multidrug resistance (MDR) proteins (P-gp and MRPs) mediated chemoresistance have been considered as a major cause of treatment failure in treatment of RB. Ocular cells have shown good tolerability against moxifloxacin (MFX). Hence, the aim of present study was to investigate the effect of moxifloxacin on the functionality of MDR proteins. Furthermore, we have also examined an interaction of MFX with anticancer agents (topotecane, etoposide and vinblastine) for RB treatment. For interaction of MFX with efflux transporter, model cell lines transfected with the efflux transporters (MDCK-MDR1 and MDCK-MRP2) were used to perform uptake and bi-directional transport experiments. Modulation of anticancer induced cell cytotoxicity, pro-inflammatory cytokines (IL-6 and IL-8) release and caspase-3 enzyme activity in presence of MFX was also evaluated. Result indicates that MFX is a substrate of both MDR1 and MRP2 efflux transporters. Furthermore elevation of anticancer uptake and bi-directional transport, reduction in IC50 cytotoxic value and modulation of antiproliferative and cytokines release in presence of MFX by anticancer agents was observed. Our results demonstrate that MFX may not only modulate the permeability of anticancer agents at efflux sites but it may also potentiate antiproliferative activity of anticancer agents in retinoblastoma cells. This study may be further extended to explore *in vivo* outcome of this finding.

Keywords

Moxifloxacin; multidrug resistant (MDR); retinoblastoma; anticancer agents

1. Introduction

Retinoblastoma is a major vision threatening intraocular malignancy affecting 300 children per year in the USA (Broaddus et al., 2009). About 80% of the children are diagnosed with retinoblastoma at less than 5 year of age. Overall, retinoblastoma makes 3% of all childhood cancers diagnosed within 15 years of age (Chintagumpala et al., 2007). The histological event includes development of retinoblastoma from immature retinal cells followed by replacement of healthy retinal tissues. Retinoblastoma displays elevated rate of apoptotic

*Corresponding author: **Ashim K. Mitra, Ph.D.**, University of Missouri Curators' Professor of Pharmacy, Chairman, Pharmaceutical Sciences, Vice-Provost for Interdisciplinary Research, University of Missouri - Kansas City, School of Pharmacy, 2464 Charlotte Street, Kansas City, MO 64108, USA, Phone: 816-235-1615, Fax: 816-235-5779, mitraa@umkc.edu.

and tumor turnover events which leads to ocular necrosis and dystrophic calcification (Chintagumpala et al., 2007). The most common symptoms of retinoblastoma include leukocoria (white discoloration in pupil) and strabismus (ocular misalignment) (Shields and Augsburger, 1981; Shields et al., 1991).

Chemotherapy is the key retinoblastoma treatment to reduce tumor size and to facilitate local therapies (cryotherapy, laser photocoagulation or thermotherapy) for eradication of the disease-causing cells (Chintagumpala et al., 2007). The commonly used chemotherapeutic agents include carboplatin, topotecan, etoposide, and vinblastine. These agents suffer from poor cell permeability and chemo-resistance due to major interaction with multidrug resistant (MDR) efflux proteins (Chen et al., 1996; Horowitz et al., 2004; Rautio et al., 2006). Innate expression of several efflux proteins such as P-glycoprotein (P-gp/MDR1), multidrug resistant proteins (MRPs), and lung resistance protein are reported on the retinoblastoma tumor (Chan et al., 1997; Chan et al., 1991; Krishnakumar et al., 2004; Wilson et al., 2009). Over-expression of cell membrane-based efflux transporters play an important role in drug resistance by restricting intracellular entry of therapeutic drugs used in a clinical setting. Many scientists have utilized different efflux pump evasion strategies to overcome drug resistance for improving drug intracellular permeability (Gokulgandhi et al.; Jain et al., 2005). One of such strategies involves co-administration of MDR1/MRP inhibitors to increase intracellular accumulation of therapeutic substrates (Chan et al., 1996; Dimaras et al.; Lee et al., 1993). However, utilization of efflux pump inhibitors has its own limitations as (i) it is not clinically approved, (ii) causes undesirable clinical pharmacokinetic interactions including interaction with major drug metabolizing enzymes (Pal and Mitra, 2006; Wang et al., 2008), and (iii) little or no additional improvement in the therapeutic activity of drug. In the present report, we intend to study drug interaction strategy to simultaneously overcome chemo-resistance and to improve anticancer activity for retinoblastoma tumor.

Moxifloxacin is a promising fourth generation fluoroquinolone that exhibits broad spectrum of antimicrobial activity against both gram-positive as well as gram-negative microorganisms. Moxifloxacin generates bactericidal activity by binding to essential bacterial enzymes (topoisomerase II or DNA gyrase and topoisomerase IV) and thereby interferes with the bacterial DNA replication, transcription, and repair mechanism (Callegan et al., 2003; Saravolatz and Leggett, 2003; Scoper, 2008). Fluoroquinolone moxifloxacin is approved for various respiratory tract (acute sinusitis, chronic bronchitis, and community-acquired pneumonia) and ocular (bacterial conjunctivitis) infections (Benitez-Del-Castillo et al.; Saravolatz and Leggett, 2003).

Ocular cells (corneal endothelial cells, primary human trabecular meshwork and retinal pigment epithelial cells) have shown good tolerability against clinically accepted moxifloxacin even at higher dose levels (concentration up to 500 μg/mL (1.24 mM) for 30 days) (Kernt et al., 2009; McGee et al., 2005). Besides bactericidal activity, moxifloxacin mediated anti-topoisomerase II activity in eukaryotic and tumor cells have been reported (Bromberg et al., 2003). Moreover, moxifloxacin mediated enhanced anti-topoisomerase I and cytotoxic activity of chemotherapeutic agents in tumor derived cell lines have been observed (Fabian et al., 2006; Reuveni et al., 2008). Moxifloxacin has further shown inhibition of anticancer mediated release of pro-inflammatory mediators (IL-8, IL-1b and TNF-a) in THP-1 and Jurkat cells (Fabian et al., 2006; Weiss et al., 2004). Immunomodulatory and protective effects of moxifloxacin against bacterial strains have proposed its potential for treating patients undergoing chemotherapy and immune suppression (Dalhoff and Shalit, 2003; Shalit et al., 2002; Shalit et al., 2001). Anti-angiogenic effects of moxifloxacin in combination with anticancer agent following

spontaneous or drug induced release of pro-angiogenic cytokines have further suggested it as a potential therapeutic agent for treating cancerous diseases (Reuveni et al.).

In addition to anticancer agents, fluoroquinolones can also exhibits efflux pump mediated acquired drug resistance (Asbell et al., 2008; Barot et al.; Bertino, 2009). Therefore, it is important to delineate the interaction of moxifloxacin with major efflux transporters. P-glycoprotein (MDR1) and multidrug resistance protein 2 (MRP2) belongs to the ATP-binding cassette transporter super family and act as energy-dependent efflux pumps. These efflux proteins hinder intracellular drug entry and reduce drug concentration inside the cells. Moreover, based on the above literature findings which suggest a potential role of moxifloxacin in modulating activity of cytotoxic agents, it would be interesting to study its interaction with anticancer agents for the management of retinoblastoma.

In this report, we present the interaction of moxifloxacin with major efflux transporters (MDR1 and MRP2) and anticancer agents (topotecan, etoposide, vinblastine) currently used for the treatment of retinoblastoma. Anticancer topotecan, etoposide and vinblastine are known substrate of MDR1 and MRP2 efflux transporters. We hypothesized that in such interactions, moxifloxacin will not only modulate the permeability of anticancer agent across retinoblastoma cells expressing efflux proteins (due to competitive inhibition at efflux sites) but it will also enhance the cytotoxic activity of chemotherapeutics. Series of experiments presented below have been performed to investigate above hypothesis.

Materials and methods

2.1 Materials

MDCK-WT (wild-type) cells and MDCK cells transfected with the human MDR1 (MDCK-MDR1) and MRP2 (MDCK-MRP2) genes were generously provided by Drs. Alfred H. Schinkel and Piet Borst (The Netherlands Cancer Institute, Amsterdam, Netherlands) and human retinoblastoma (Y-79) and retinal pigment epithelial (ARPE-19) cells were obtained from American Type Culture Collections (ATCC; Manassas, VA, USA). Fetal bovine serum (FBS; heat inactivated and non-heat inactivated) was purchased from Atlanta Biologicals (Lawrenceville, GA, USA). Dulbecco's modified eagle medium (DMEM, for MDCK-WT, -MDR1 and -MRP2 cells), D-MEM/F-12 (for ARPE-19 cells), RPMI 1640 (for Y-79 cells) and non-essential amino acids (NEAA) were obtained from Gibco (Invitrogen, Grand Island, NY, USA). Streptomycin, penicillin, sodium bicarbonate, HEPES, etoposide, vinblastine sulfate, topotecan hydrochloride, lipopolysaccharide (LPS) and dithiothreitol (DTT) and all other chemicals were purchased from Sigma-Aldrich (St. Louis, MO, USA). Culture flasks (75 cm^2 growth area), 12-well (3.8 cm^2 growth area per well) and 96-well (0.32 cm^2 growth area per well) culture plates were obtained from Corning Costar Corp (Cambridge, MA, USA).

GF120198 was a generous gift from Glaxo SmithKline Ltd and MK571 was procured from Biomol International (Plymouth Meeting, PA, USA). [^{14}C]-Erythromycin (specific activity: 53.8 mCi/nmol) was procured from PerkinElmer Life Sciences (Boston, MA, USA). [^{3}H]-Etoposide (specific activity: 480 mCi/mmol), [^{3}H]-Topotecan (specific activity: 1.9 Ci/mmol) and [^{3}H]-Vinblastine (specific activity: 1 Ci/mmol) were purchased from Moravek Biochemicals, Inc. (Brea, CA, USA). Levofloxacin and Moxifloxacin HCl were acquired from TCI America (Sunnyvale, CA, USA) and China respectively. CellTiter 96® AQueous non-radioactive cell proliferation assay kit was obtained from Promega Corporation (Madison, WI, USA). Bradford protein assay reagent and Annexin V/propidium iodide (PI) apoptosis detection kit was purchased from Bio-Rod Laboratories (Hercules, CA, USA) and BD Pharmingen (San Diego, CA, USA) respectively. All the solvents were of HPLC grade and obtained from Fisher Scientific (St. Louis, MO).

2.2 Cell culture

MDCK-WT, MDCK-MDR1 and MDCK-MRP2 cells (passages 5–15) were cultured in DMEM supplemented with 10% FBS (heat inactivated), 1% NEAA, penicillin (100 U/mL), streptomycin (100 μg/mL), 20 mM HEPES, 29 mM sodium bicarbonate and adjusted to pH 7.4. Human retinoblastoma cells (Y-79) were incubated in 75 cm^2tissue culture flasks as a suspension in RPMI 1640 medium supplemented with 15% non-heat inactivated FBS, 1 mM glutamine, penicillin (100 units/mL) and streptomycin (100 μg/mL). Human retinal pigment epithelium (ARPE-19) cells (passages 20–30) were cultured in D-MEM/F-12 supplemented with 10% heat-inactivated FBS, 15 mM HEPES, 29 mM sodium biocarbonate, penicillin (100 units/mL), streptomycin (100 μg/mL).

All the cell lines were grown and incubated at 37°C with 5% $CO^2$and 90% relative humidity. The medium was changed every alternate day and cells were passaged upon reaching 80%–90% confluency. For uptake experiments, cells were seeded at a density of 25000 per well in 2 mL of medium in 12-well tissue culture plates. For transport experiments, the collagen-coated Transwell® permeable inserts (Costar®) were plated at a density of 25000 cells per well in 12-well tissue culture plates. The apical (AP) and basolateral (BL) side of cells were treated with 0.5 mL and 1.5 mL of medium respectively.

2.3 Cellular accumulation of [^{14}C]-erythromycin

Uptake studies were performed according to the previously published protocol (Barot et al.; Gokulgandhi et al.). Briefly, MDCK-MDR1 and MDCK-MRP2 cell monolayer was washed (3 × 10 min) with Dulbecco's Phosphate-Buffered Saline (DPBS) pH 7.4. [^{14}C]-erythromycin has been widely applied as a radiolabeled MDR1 and MRP2 substrate and can be detected in very low concentrations (Reuveni et al.). The uptake of [^{14}C]-erythromycin (0.25 μCi/mL) was initiated alone or in presence of moxifloxacin (500 μM), GF120198 (2 μM) and MK571 (50 μM) in DPBS (pH 7.4) onto the cell monolayer at 37 °C. After 30 min incubation, the donor solution was removed and cells were immediately washed with ice-cold stop solution (200 mM KCl and 2 mM HEPES) three times. Cells were lysed with 1 mL lysis solution (0.1% w/v Triton X-100 in 0.3 N sodium hydroxide) and kept overnight at room temperature. The next day, 500 μL of cell lysate was transferred to scintillation vials containing 3 mL scintillation cocktail. Finally, samples were analyzed by Beckman Scintillation Counter (Model LS-6500, Beckman Instruments, Inc.). Uptake was normalized to the protein content of each well. Protein content of cell lysate was quantified using Bradford reagent. Uptake experiments were performed in quadruplicate (n = 4).

Following a similar procedure, the inhibitory potential of moxifloxacin against MDR1 and MRP2 mediated [^{14}C]-erythromycin efflux was determined. [^{14}C]-erythromycin (in DPBS pH 7.4, 0.25 μCi/mL) was spiked with increasing concentrations of moxifloxacin (0.1 μM – 1mM) in MDCK-MDR1 and MDCK-MRP2 cells. Data was fitted to calculate the half maximal inhibitory concentration (IC_{50}) from the modified log [dose]-response curve.

2.4 Bi-directional transport of [^{14}C]-erythromycin

Bi-directional transport experiments of [^{14}C]-erythromycin were performed using Transwell® diffusion chamber system according to the previously published protocol (Gokulgandhi et al.). MDCK-WT, MDCK-MDR1 and MDCK-MRP2 cell monolayers grown on the Transwell® inserts were rinsed and incubated with DPBS (pH 7.4) at 37 °C (2 × 10 min) for both AP and BL sides. AP to BL transport was initiated by adding 500 μL of [^{14}C]-erythromycin (in DPBS pH 7.4, 0.5 μCi/mL) alone and in presence of moxifloxacin (500 μM in DPBS pH 7.4), GF120918 (2.0 μM) or MK571 (50 μM) towards AP side of cells (donor chamber) where, receiver chamber (BL side) contains DPBS (pH 7.4). Similarly, BL to AP transport was initiated by adding 1500 μL of [^{14}C]-erythromycin alone and in

presence of moxifloxacin, GF120918 or MK571 toward BL side of cells (donor chamber), where AP side of cells was treated as the receiver chamber. Cell monolayer integrity (around 250 Ωcm^2) was determined by transepithelial electrical resistance (TEER) measurement. Bi-directional transport was conducted for 3 h. Sampling (100 μL) from the receiver chamber was conducted at predetermined time intervals of 15, 30, 45, 60, 90, 120, 150, and 180 min. Fresh DPBS (pH 7.4) was replaced to maintain the sink conditions in the receiver chamber. Samples (n = 3) were analyzed by Beckman Scintillation Counter (Model LS-6500, Beckman Instruments, Inc.).

2.5 Bi-directional transport of moxifloxacin

Bi-directional transport of moxifloxacin was performed as described previously. AP to BL transport was initiated by adding 500 μL of moxifloxacin (in DPBS pH 7.4, 500 μM) alone and in presence of GF120918 (2.0 μM) or MK571 (50 μM) towards AP side of cells (donor chamber) where, receiver chamber (BL side) contains DPBS (pH 7.4). Similarly, BL to AP transport was initiated by adding 1500 μL of moxifloxacin (in DPBS pH 7.4, 500 μM) alone and in presence of GF120918 or MK571 toward BL side of cells (donor chamber), where AP side of cells were treated as a receiver chamber. Samples (n = 4) were analyzed by LC–MS/MS after cold ethyl acetate extraction (refer supplementary information). Extracted samples were evaporated in speed vacuum and reconstituted in optimized mobile phase.

2.6 Cellular accumulation of anticancer agents

Uptake studies were performed according to the previously published protocol (Barot et al.; Gokulgandhi et al.). Briefly, MDCK-MDR1 and MDCK-MRP2 cell monolayer was washed (3×10 min) with DPBS (pH 7.4). The uptake of [^{3}H]-Etoposide, [^{3}H]-Topotecan and [^{3}H]-Vinblastine (each 0.25 μCi/mL) was initiated alone or in presence of moxifloxacin (500 μM) in DPBS pH 7.4 (for etoposide and vinblastine) or pH 5.5 (for topotecan) onto the cell monolayer. The uptake was performed at different time point (15, 30 and 60 min) at 37 °C. Following incubation, the donor solution was removed and cells were immediately washed with ice-cold stop solution for 3 times.

Cells were lysed with 1mL lysis solution and kept overnight at room temperature. Next day, 500 μL of cell lysate was transferred in to scintillation vials containing 3 mL scintillation cocktail. Finally, samples were analyzed by Beckman Scintillation Counter (Model LS-6500, Beckman Instruments, Inc.). Uptake was normalized to the protein content of each well. Protein content of cell lysate was quantified using Bradford reagent. Uptake experiment was performed in quadruplicate (n=4).

2.7 Bidirectional transport of anticancer agents

Bi-directional transport of [^{3}H]-Etoposide, [^{3}H]-Topotecan and [^{3}H]-Vinblastine was performed according to the previously described method. AP to BL transport was initiated by adding 500 μL (0.5μCi/mL) of [^{3}H]-Etoposide (in DPBS pH 7.4), [^{3}H]-Vinblastin (in DPBS pH 7.4) and [^{3}H]-Topotecan (in DPBS pH 5.5) alone and in presence of moxifloxacin (500 μM), GF120918 (2.0 μM) or MK571 (50 μM) towards AP side of cells (donor chamber) where, receiver chamber (BL side) contains DPBS (pH 7.4). Similarly, BL to AP transport was initiated by adding 1500 μL (0.5μCi/mL) of [^{3}H]-Etoposide, [^{3}H]-Vinblastin and [^{3}H]-Topotecan alone and in presence of moxifloxacin, GF120918 or MK571 toward BL side of cells (donor chamber), where AP side of cells were treated as a receiver chamber. Samples (n=3) were analyzed by Beckman Scintillation Counter (Model LS-6500, Beckman Instruments, Inc.).

2.8 Anti-proliferative activity

Previously published protocol was followed with modification (Vene et al., 2007). Y-79 cells (5×10^5) were seeded in 1 mL of culture medium/well in a 24-well plate. Y-79 cells were treated with various concentrations of etoposide (1–40 μM), vinblastine (1–40 nM) and topotecan (1–40 μM) alone and in presence of moxifloxacin (500 μM) for different time points (48 and 72 h at 37 °C with 5% $CO^2$and 90% relative humidity). Following incubation, 100 μL MTT (5 mg/mL in PBS) per 1 mL medium was added to the cells and further incubated for 2–3 h. Cells were centrifuged at 5000 rpm and cell pellets were dissolved in 100 μL of DMSO. The optical density of cell suspension (n = 6) was measured at 485 nM using 96-well microtiter plate reader (SpectraFluor Plus, Tecan, Switzerland). Cells suspended in culture medium were treated as a control. IC_{50} values of anticancer agents were calculated from nonlinear regression analysis using GraphPad Prism Software version 5.0 (GraphPad Software Inc., San Diego, CA). Data were plotted as percentage viable cells against anticancer drug concentrations.

2.9 Caspase-3 assay

Caspase-3 release was measured according to the previously published protocol with modification (Fabian et al., 2006). Briefly, Y-79 cells were incubated (24 h) with different concentrations (1, 5 and 10 μM) of anticancer agent (etoposide, topotecan and vinblastine) alone and in presence of moxifloxacin (500 μM). Following incubation, cells were washed and resuspended in 50 mM HEPES (pH 7.4), 0.1% Triton X-100, DTT (5 mM), EDTA (0.1 mM) and incubated on ice for 15 min. Cells were lysed by three successive freeze–thaw cycles (dry ice/37 °C). The cell lysates were centrifuged at 12000 rpm (15 min, 4 °C) and the supernatants were stored at −80 °C until further analysis. The protein concentration of each sample was estimated using Bradford Bio-Rad protein assay. To determine caspase-3 activity, 25 μg protein was incubated in dark (37°C, 60 min) with 30 mM Ac-DEVD-AMC (caspase-3 substrate with Km = 9.7 μM; Anaspec, San Jose, CA). Ac-DEVD is a caspase-specific peptide that is conjugated to the fluorescent reporter molecule 7-amino-4-methyl coumarin (AMC). Caspase mediated cleavage of peptide releases fluorochrome (AMC) which was measured at 360 nM (excitation) and 460 nM (emission) wavelengths.

2.10 Apoptosis assay

Y-79 cell apoptosis was measured by flow cytometry after concurrent staining with annexin-V FITC and propidium iodide (PI) (Fabian et al., 2006; Gruss-Fischer and Fabian, 2002). Briefly, Y-79 cells were incubated with anticancer agent alone or in presence of moxifloxacin for 24 h. Following incubation, cells were washed with cold PBS and resuspended in annexin V-PI binding buffer (10 mM HEPES pH 7.4, 140 mM NaCl, 2.5 mM $CaCl_2$). An aliquot of 100 μL was mixed with 4 mL of annexin-V FITC and PI. The mixture was incubated for 15 min at room temperature in the dark. Finally, cells were washed and resuspended in binding buffer and subjected to flow cytometric analysis on FACScan (Becton Dickinson, Franklin Lakes, NJ, USA).

2.11 Pro-inflammatory cytokines assay

Anticancer mediated release of IL-6 and IL-8 from ARPE-19 cells were quantified according to the previously published protocol with modification (Wu et al.). Briefly, ARPE-19 cells suspended in DMEM/F12 medium were placed in 24-well culture plates at a concentration of 1×10^6cells per mL. Cells were incubated (48 h) with two different concentrations (0.5 and 1.0 μg/mL) of anticancer agent alone and in presence of moxifloxacin (500 μM/20 μg). Following drug exposure, cell-free supernatants were recovered and cytokines concentrations were determined using Legend Max® human IL-6 and IL-8 sandwich ELISA kit (BioLegend®, San Diego, CA) according to the manufacturer

protocol. IL-6 and 8 standard controls (100 pg/mL - 3.125 pg/mL), negative control (cell culture medium), positive control (lipopolysaccharide (LPS)) were also quantified simultaneously. Absorbance was measured at 450 nM (excitation) and 570 nM (emission) wavelengths.

2.12 Data treatment

For dose–response studies, the effect of moxifloxacin on [^{14}C]-erythromycin efflux was calculated using a modified log [dose]-response curve method to fit the data in equation 1 in order to obtain IC_{50} values,

$$Y=[\mathrm{Min}+\frac{\max-\min}{1+10^{(\log IC50-x)*H}}] \quad \text{Eq. 1}$$

where **x** denotes the log concentration of moxifloxacin, **Y** is the cellular accumulation of [^{14}C]-erythromycin, IC_{50} represents the inhibitor concentration where the efflux of [^{14}C]-erythromycin is inhibited by 50%, and **H** is the Hill constant. **Y** starts at a minimum (min) value (at low inhibitor concentration) and then plateaus at a maximum (max) value (at high inhibitor concentration) resulting in a sigmoidal curve.

Cumulative amounts transported in bi-directional transport experiments across cell monolayers were plotted as a function of time. Linear regression of amounts transported as a function of time yielded the rate of transport across the cell monolayer (dM/dt). Rate divided by the cross-sectional area available for transport (A) generated steady state flux as shown in Eq. 2.

$$\mathrm{Flux}=(\frac{dM}{dt})/A \quad \text{Eq. 2}$$

Slopes were obtained from the linear portion of the curve to calculate apparent permeability (Papp) through normalization of the steady-state flux to the donor concentration (Cd) according to Eq. 3.

$$\mathrm{Papp}=\frac{dM/dt}{(Cd*A*60)} \quad \text{Eq. 3}$$

When a dM/dt (mol/min) represents the rate of drug transport across the cell monolayer, A (cm^2) is the cross-sectional area available for transport, and Cd (μM) is the donor concentration. The net efflux ratio was assessed from Papp in BL to AP and AP to BL directions as shown in Eq. 4.

$$\mathrm{Efflux\ \ Ratio}=(\mathrm{PappBL}\rightarrow\mathrm{AP})/(\mathrm{PappAP}\rightarrow\mathrm{BL}) \quad \text{Eq. 4}$$

2.13 Statistical analysis

All the results are expressed as mean ± standard deviation (SD). The student t test was applied to determine statistical significance between two groups where, $p < 0.05$ being considered statistically significant.

2. Results

3.1 Cellular accumulation of [^{14}C]-erythromycin

Cellular accumulation of [^{14}C]-erythromycin was significantly ($P \leq 0.05$) elevated in the presence of GF120918 (193%) and MK571 (273%) relative to control on MDCK-MDR1 and MDCK-MRP2, respectively (Fig. 1). In the presence of moxifloxacin, cellular accumulation of [^{14}C]-erythromycin was increased by 150% and 220% on MDCK-MDR1 and MDCK-MRP2 cells, respectively (Fig. 1).

Dose-dependent inhibition of [^{14}C]-erythromycin efflux was observed in presence of increasing concentration of moxifloxacin on MDCK-MDR1 and MDCK-MRP-2 cells, respectively (Fig. 2). A modified log [dose]-response curve was applied to fit the data in order to obtain IC_{50} values. From the dose-response curve, moxifloxacin IC_{50} values against MDR1 and MRP2 mediated inhibition of [^{14}C]-erythromycin efflux was 217 μM and 187 μM, respectively.

3.2 Bi-directional transport of [^{14}C]-erythromycin

The apparent permeability of [^{14}C]-erythromycin across MDCK cells overexpressing MDR1 and MRP2 proteins was significantly higher in the BL-AP direction relative to the AP-BL direction (Table S1) due to the expression of these transporters on the apical side of the cells. For MDCK-MDR1 cells, the BL-AP and AP-BL permeabilities of [^{14}C]-erythromycin were $18.83 \pm 1.05 \times 10^{-6}$and $5.44 \pm 0.52 \times 10^{-6}$cm/s, respectively, leading to an efflux ratio of 3.46. Similarly, BL-AP and AP-BL permeabilities of [^{14}C]-erythromycin across MDCK-MRP2 cells were $2.70 \pm 0.18 \times 10^{-6}$and $0.62 \pm 0.13 \times 10^{-6}$cm/s, respectively, leading to an efflux ratio of 4.35. However, in the presence of moxifloxacin a significant reduction in the efflux ratio of [^{14}C]-erythromycin was observed across MDCK-MDR1 (1.71) and MDCK-MRP2 (1.92) cells due to the elevation of AP-BL permeabilities ($9.50 \pm 1.55 \times 10^{-6}$ and $1.34 \pm 0.17 \times 10^{-6}$) across both the cell lines, respectively (Table S1). Moreover, similar efflux ratio reduction (1.14 and 1.36) of [^{14}C]-erythromycin was also observed in the presence of known MDR1 (GF120918) and MRP2 (MK571) inhibitors across MDCK-MDR1 and MDCK-MRP2 cells, respectively (Table S1).

3.3 Bi-directional transport of moxifloxacin

Similar to [^{14}C]-erythromycin, the apparent permeability of moxifloxacin across MDCK-MDR1 and MDCK-MRP2 cells was significantly elevated in BL-AP direction relative to AP-BL direction (Table I) suggesting moxifloxacin is a substrate for MDR1 and MRP2 efflux transporters. For MDCK-MDR1 cells, the BL-AP and AP-BL permeabilities of moxifloxacin were $20.46 \pm 2.26 \times 10^{-6}$ and $5.81 \pm 0.44 \times 10^{-6}$ cm/s, respectively, leading to an efflux ratio of 3.52. Similarly, BL-AP and AP-BL permeabilities of moxifloxacin across MDCK-MRP2 cells were $1.97 \pm 0.41 \times 10^{-6}$ and $0.78 \pm 0.13 \times 10^{-6}$ cm/s, respectively, leading to an efflux ratio of 2.53. Moreover, reduction of moxifloxacin efflux ratio was observed in the presence of known MDR1 (1.25) and MRP2 (1.20) inhibitors across MDCK-MDR1 and MDCK-MRP2 cells, respectively (Table I).

3.4 Cellular accumulation of anticancer agents

Time and concentration dependent increased cellular accumulation of anticancer agents were observed in presence of moxifloxacin. Highest cellular accumulation of [^{3}H]-etoposide, [^{3}H]-vinblastine and [^{3}H]-topotecan was observed at 60 min in presence of moxifloxacin (500 μM) across MDCK-MDR1 (189.15 ± 5.41 %, 210.78 ± 10.46 % and 199.95 ± 11.26%; n=4 each) and MDCK-MRP2 (263.71 ± 14.97 %, 189.78 ± 10.46 % and 212.95 ± 11.26 %; n=4 each) cells, respectively (Fig. 3).

3.5 Bidirectional transport of anticancer agents

Apparent permeabilities of all three anticancer agents were significantly higher in BL-AP direction in presence of moxifloxacin across MDCK-MDR1 and MDCK-MRP2 cells (Table II). The efflux ratio of [^{3}H]-etoposide was 3.25 (Papp AP→BL = (3.57 ± 0.65) × 10^{-6} cm/s) and 5.46 (Papp AP→BL = (37.82 ± 2.70) × 10^{-6} cm/s) across MDCK-MDR1 and MDCK-MRP2 cells, respectively. Significant reduction of [^{3}H]-etoposide efflux ratio was observed due to the elevation of AP-BL permeability in presence of moxifloxacin across MDCK-MDR1 (1.62, Papp AP→BL = (7.92 ± 1.78) × 10^{-6} cm/s) and MDCK-MRP2 (2.17, AP→BL = (89.34 ± 1.75) × 10^{-6} cm/s) cells. Moreover, [^{3}H]-etoposide efflux ratio reduction (1.03 and 1.08) was also observed in presence of known MDR1 (GF120918) and MRP2 (MK571) inhibitors across MDCK-MDR1 and MDCK-MRP2 cells, respectively (Table II). Similarly, efflux ratio of [^{3}H]-vinblastine was 6.59 (Papp AP→BL = (1.55 ± 0.03) × 10^{-6} cm/s) and 5.46 (Papp AP→BL = (13.50 ± 3.24) × 10^{-6} cm/s) across MDCK-MDR1 and MDCK-MRP2 cells, respectively. Significant reduction of [^{3}H]-vinblastine efflux ratio was observed due to the elevation of AP-BL permeability in presence of moxifloxacin across MDCK-MDR1 (2.26, AP→BL = (3.95 ± 0.46) × 10^{-6} cm/s) and MDCK-MRP2 (2.48, AP→BL = (19.72 ± 2.56) × 10^{-6} cm/s) cells. Furthermore, [^{3}H]-vinblastine efflux ratio reduction was also observed in presence of GF120198 (1.33) and MK571 (1.39) across MDCK-MDR1 and MDCK-MRP2 cells, respectively (Table II). The efflux ratio of [^{3}H]-topotecan was 4.63 (Papp AP→BL = (0.75 ± 0.03) × 10^{-6} cm/s) and 3.07 (Papp AP→BL = (8.06 ± 0.66) × 10^{-6} cm/s) across MDCK-MDR1 and MDCK-MRP2 cells, respectively. Significant reduction of [^{3}H]-topotecan efflux ratio was observed in presence of moxifloxacin across MDCK-MDR1 (2.16, Papp AP→BL = (1.56 ± 0.03) × 10^{-6} cm/s) and MDCK-MRP2 (1.80, Papp AP→BL = (12.67 ± 2.67) × 10^{-6} cm/s) cells. Likewise, [^{3}H]-topotecan efflux ratio reduction was also observed in presence of GF120198 (1.38) and MK571 (1.13) across MDCK-MDR1 and MDCK-MRP2 cells, respectively (Table II).

3.6 Anti-proliferative activity

Cytotoxicity of anticancer agents against retinoblastoma cells (Y-79) was measured alone and in presence of moxifloxacin for different time points using the MTT assay. Significant reduction in % cell viability was observed upon co-exposure of anticancer drug and moxifloxacin relative to treatment of anticancer drug alone (Fig. 4). Based on cytotoxicity results, IC_{50} value of anticancer agents were calculated alone and in presence of moxifloxacin. The IC_{50} value of etoposide (27.07 μM), topotecan (27.89 μM) and vinblastine (51.90 nM) against retinoblastoma cells were significantly reduced to 2.11 μM, 2.89 μM and 22.92 nM, respectively in presence of moxifloxacin.

3.7 Caspase-3 assay

Concentration dependant caspase-3 release was observed in response to anticancer drug treatment which was further increased up to 1.6 (etoposide), 2.9 (topotecan) and 6.6 (vinblastine) fold in presence of moxifloxacin (Fig. 5).

3.8 Apoptosis assay

Anticancer concentrations equivalent to IC_{50} values (calculated from cytotoxicity studies) in presence or absence of moxifloxacin were exposed to Y-79 cells for 24 h. Live and dead cell discrimination was measure by flow cytometry analysis using Annexin-V FITC-PI dual staining. The % cell population in early apoptotic (Annexin-V positive and PI negative) and necrosis/late apoptotic (Annexin-V positive and PI positive) stages were nearly similar when Y-79 cells were treated with equivalent concentration of etoposide (27 or 2.1 μM) (Fig. 6),

topotecan (28 or 2.8 μM) (Fig. 6) and vinblastine (50 or 23 nM) (Fig. 6) alone or in combination with moxifloxacin, respectively.

3.9 Pro-inflammatory cytokine assay

Dose-dependent anticancer mediated cytokine release (IL-6 and IL-8) was observed in retinal cells (ARPE 19). After 48 h exposure of etoposide (0.5 and 1.0 μg) on Y-79 cells, release of IL-6 (105.20 ± 3.90, 151.40 ± 10.00 pg mL^{-1}) and IL-8 (191.90 ± 9.10, 286.60 ± 16.60 pg mL^{-1}) was reduced by 1.3, 1.4 (for IL-6) and 1.60, 1.28 (for IL-8) fold in presence of moxifloxacin, respectively (Fig. 7). Similarly, vinblastine (0.5 and 1.0 μg) mediated release of IL-6 (52.90 ± 4.30, 73.60 ± 2.30 pg mL^{-1}) and IL-8 (140.20 ± 14.40, 284.90 ± 18.00 pg mL^{-1}) was reduced by 1.11, 1.42 (for IL-6) and 1.40, 1.08 (for IL-8) fold in presence of moxifloxacin, respectively (Fig. 7). In case of topotecan (0.5 and 1.0 μg), release of IL-6 (156.90 ± 2.70, 157.50 ± 8.80 pg mL^{-1}) and IL-8 (157.70 ± 12.60, 239.20 ± 13.90 pg mL^{-1}) was reduced by 1.3 and 1.2 (for IL-6) and 1.48, 1.30 (for IL-8) fold in presence of moxifloxacin, respectively (Fig. 7).

3. Discussion

Moxifloxacin is a potent fluoroquinolone antibiotic used in the clinical settings for the treatment of respiratory and ocular infections (Benitez-Del-Castillo et al.; Saravolatz and Leggett, 2003). Besides bacterial drug resistance, MDR represents a major barrier to clinically successful fluoroquinolone therapy. Majority of fluoroquinolones are reported to be substrates of MDR efflux proteins which significantly reduces its intracellular accumulation and bioavailability (Barot et al.). Therefore, primary objective of this report was to evaluate interaction of moxifloxacin with major efflux transporters (MDR1 and MRP2) to delineate effect of MDR proteins on intracellular translocation of moxifloxacin.

Previous report indicates that erythromycin can be selected as a model substrate to study MDR1 and MRP2 mediated efflux (Hariharan et al., 2009). Therefore, a preliminary interaction experiment was carried out by studying cellular accumulation of erythromycin in the presence of moxifloxacin in MDCK-MDR1 and MDCK-MRP2 cells. Cellular accumulation of [^{14}C]-erythromycin appears to be significantly higher in presence of GF120918 (known MDR1 inhibitor) and MK571 (known MRP2 inhibitor) relative to control in MDCK-MDR1 and MDCK-MRP2 cells, respectively (Fig. 1) confirming an excellent MDR1 and MRP2 substrate specificity of [^{14}C]-erythromycin (Hariharan et al., 2009). Significantly higher cellular accumulation of [^{14}C]-erythromycin in presence of moxifloxacin across both the cell lines indicates moxifloxacin interacts with MDR1 and MRP2, suggesting moxifloxacin substrate specificity for both efflux transporters.

Furthermore, dose-dependent inhibitions of [^{14}C]-erythromycin efflux suggest high affinity of moxifloxacin towards MDR1 and MRP2 efflux transporters (Fig. 2). IC_{50} values indicates higher affinity of moxifloxacin towards MRP2 (187 μM) relative to MDR1 (217 μM) efflux transporter. This observation suggests that inhibitory potential of moxifloxacin for MDR1 and MRP2 mediated [^{14}C]-erythromycin efflux was competitive in nature.

Apical localization of MDR1 and MRP2 efflux transporters on the MDCK-MDR1 and MDCK-MRP2 cells exhibited much higher [^{14}C]-erythromycin transport in AP-BL direction relative to BL-AP direction (Table S1). A significant elevation of AP-BL transport of [^{14}C]-erythromycin in presence of moxifloxacin across both the cell lines confirms the substrate specificity of moxifloxacin towards MDR1 and MRP2. Since, reduction of efflux ratio value to 1.0 leads to equivalent transport in both the direction. Significant reduction of [^{14}C]-erythromycin efflux ratio in presence of moxifloxacin confirms competitive inhibition of MDR1 and MRP2 functional activities. Furthermore, AP-BL permeability of moxifloxacin

increased by 2.80 and 2.10 times in presence of GF120918 and MK571, respectively (Table I). This permeability escalation has led to moxifloxacin efflux ratio reduction in MDCK-MDR1 and MDCK-MRP2 cells. This observation further confirms the substrate specificity of moxifloxacin towards MDR1 and MRP2 efflux transporters. This overlapping substrate specificity of moxifloxacin for MDR1 and MRP2 may endure a synergistic efflux action and may develop resistance by lowering intracellular concentration and permeability of moxifloxacin. Therefore, it is suggested that attention must be given to the eventual consequences of moxifloxacin interaction with efflux transporters and strategies should be developed to circumvent MDR1 and MRP2 mediated moxifloxacin resistance. Furthermore, co-administration of moxifloxacin with therapeutic substrate of these efflux transporters such as erythromycin may inhibit efflux of later due to competitive inhibition of MDR1 and MRP2. This may ultimately improve the intracellular permeability of MDR1 and MRP2 substrates and may also lower the incidence of drug resistance. Therefore, we have further tested moxifloxacin potential to overcome efflux based drug resistance of anticancer agents (etoposide, topotecan and vinblastine) which are also overlapping substrates of MDR1 and MRP2 and currently used for retinoblastoma management. Retinoblastoma is the malignant tumors in the retinal cell layer of the eye. MDR mediated chemo-resistance due to interaction of anticancer agents with efflux proteins (MDR1 and MRP2) over-expressed on retinoblastoma tumors is the major cause of treatment failure (Chan et al., 1991; Krishnakumar et al., 2004; Wilson et al., 2009). We hypothesized that moxifloxacin being dual substrate of MDR1 and MRP2 efflux transporters may modulate the intracellular accumulation and permeability of anticancer agents due to competitive inhibition at efflux sites. This strategy might not only result in anticancer efflux modulation or inhibition, but might also result in a synergistic pharmacological effect because antimicrobial moxifloxacin has also displayed anticancer activity in eukaryotic and tumor cells (Bromberg et al., 2003; Fabian et al., 2006; Reuveni et al.; Reuveni et al., 2008). Therefore, *in vitro* experiments were conducted to test this strategy by studying cellular accumulation and bi-directional transport of anticancer agents in combination with moxifloxacin. Since, moxifloxacin and anticancer agents are overlapping substrate of MDR1 and MRP2 therefore *in vitro* uptake and transport experiments were simultaneously studied on both MDCK-MDR1 and MDCK-MRP2 cells.

Increased cellular accumulation of etoposide, topotecan and vinblastine in presence of moxifloxacin suggest competitive inhibition of MDR1 and MRP2 mediated anticancer efflux (Fig. 3). Furthermore, moxifloxacin inhibited the anticancer efflux in a dose-dependent and time-dependent manner. Since, the maximum anticancer efflux inhibition was observed at a 500 μM concentration of moxifloxacin (a non-toxic and tolerable dose), remaining studies were performed using 500 μM concentration. Elevation of AP-BL permeability of [^{3}H]-etoposide (2.22 and 2.36 fold), [^{3}H]-topotecan (2.08 and 1.57 fold) and [^{3}H]-vinblastine (2.55 and 1.46 fold) across MDCK-MDR1 (Table II) and MDCK-MRP2 (Table II) cells further confirms moxifloxacin mediated inhibition of anticancer efflux. Significant reduction of anticancer efflux ratio by moxifloxacin strongly supports co-administration of overlapping substrates as a viable strategy to overcome MDR. Overall, *in vitro* uptake and bi-directional transport studies suggest that moxifloxacin modulates the intracellular accumulation and permeability of anticancer agents.

The cytotoxicity of anticancer agents against retinoblastoma cells (Y-79) was measured alone and in presence of moxifloxacin using the MTT assay. Cytotoxicity was conducted with increasing concentration of anticancer agent (1–40 μM or 1–40 nM) at two different time points. A significant reduction of % cell viability was observed when anticancer agents and moxifloxacin were used in combination (Fig. 4). This result may be associated with the reported anti-proliferative activity of moxifloxacin (Reuveni et al., 2008). Another possible explanation for moxifloxacin mediated modulation of anticancer cytotoxicity may be due to

improved intracellular accumulation and permeability of anticancer agents (as demonstrated in *in vitro* anticancer uptake and transport studies). However, the significant reduction of etoposide (13 fold), topotecan (10 fold) and vinblastine (2 fold) IC_{50} values in the presence of moxifloxacin suggest that moxifloxacin is not only modulating the intracellular anticancer accumulation but is also elevating the cytotoxicity of the chemotherapeutic agents. Furthermore, a larger reduction in IC_{50} values for etoposide and topotecan in combination with moxifloxacin supports previously published observation that moxifloxacin alone slightly inhibits human topoisomerase II activity (Fabian et al., 2006). Previously published report has shown that combination of moxifloxacin with a topoisomerase II inhibitor (etoposide) exhibited significantly high inhibitory effect on topoisomerase II activity (Fabian et al., 2006).

Using flow cytometric analysis, the potency of calculated IC_{50} values of anticancer agents (with or without moxifloxacin) were validated. We observed a similar pattern of apoptotic events at reduced IC_{50} values of anticancer drug in presence of moxifloxacin (Fig. 6). These results showed that moxifloxacin potentiated the apoptotic effect of the anticancer agents and a similar effect can be achieved at reduced anticancer dose. This finding was further supported by measuring caspase-3 levels in Y-79 cells. Caspase-3 is the key enzyme activated during the apoptosis process and is also required for the execution of apoptotic events. The results showed that moxifloxacin alone slightly elevated caspase-3 activity; however it led to significantly high anticancer induced caspase-3 activation in dose-dependent manner (Fig. 5).

We show in the present study that treatment of ARPE-19 cells with anticancer agents induced the release of the proinflammatory cytokines IL-6 (Fig. 7) and IL-8 (Fig. 7). Recent studies have shown that IL-8 is a proangiogenic cytokine regulating tumorigenesis in DLD-1 colon cancer cells (Mizukami et al., 2005), and also serves *in vitro* as an autocrine growth factor in human colon carcinoma cells (Brew et al., 2000). These effects should be looked at as undesired side effects of the drug. Our results showed that moxifloxacin significantly inhibited the drug induced IL-8 and IL-6 release in ARPE-19 cells. This may suggest that moxifloxacin may also modulate the anticancer mediated release of proinflammatory cytokines.

4. Conclusion

In summary, above results provides direct evidence that moxifloxacin is a substrate of MDR1 and MRP2 efflux transporters. Furthermore, the drug interactions study attempted for the treatment of retinoblastoma shows triple benefit in terms of overcoming chemoresistance, enhancing cytotoxic activity and inhibiting proinflammatory cytokines release. Knowing that moxifloxacin is a clinically approved drug and exhibits tolerability in ocular cells at high concentration level and cytochrome P450 metabolizing enzyme system is not involved in its metabolism, the additional property ascribed to this drug in this manuscript may be clinically useful. There is a need to further explore this finding which may aid in the reduction of chemotherapeutic doses and associated dose-limiting toxicities. Furthermore, it is important to study and identify such interactions to further evaluate treatment options, especially when use of anticancer agent alone does not provide sufficiently robust desired clinical outcome.

Supplementary Material

Refer to Web version on PubMed Central for supplementary material.

Acknowledgments

This work was supported by NIH grants RO1 EY 09171-16, RO1 EY 10659-14 and UMKC women's council graduate assistance fund award. Authors would also like to acknowledge Dr. Anil Kumar and Ankit Shah from UMKC pharmacology department, for their guidance and support during flow cytometry analysis.

References

Asbell PA, Colby KA, Deng S, McDonnell P, Meisler DM, Raizman MB, Sheppard JD Jr, Sahm DF. Ocular TRUST: nationwide antimicrobial susceptibility patterns in ocular isolates. Am J Ophthalmol. 2008; 145:951–958. [PubMed: 18374299]

Barot M, Gokulgandhi MR, Haghnegahdar M, Dalvi P, Mitra AK. Effect of emergence of fluoroquinolone resistance on intrinsic expression of P-glycoprotein phenotype in corneal epithelial cells. J Ocul Pharmacol Ther. 27:553–559. [PubMed: 21830912]

Benitez-Del-Castillo J, Verboven Y, Stroman D, Kodjikian L. The role of topical moxifloxacin, a new antibacterial in Europe, in the treatment of bacterial conjunctivitis. Clin Drug Investig. 31:543–557.

Bertino JS Jr. Impact of antibiotic resistance in the management of ocular infections: the role of current and future antibiotics. Clin Ophthalmol. 2009; 3:507–521. [PubMed: 19789660]

Brew R, Erikson JS, West DC, Kinsella AR, Slavin J, Christmas SE. Interleukin-8 as an autocrine growth factor for human colon carcinoma cells in vitro. Cytokine. 2000; 12:78–85. [PubMed: 10623446]

Broaddus E, Topham A, Singh AD. Incidence of retinoblastoma in the USA: 1975–2004. Br J Ophthalmol. 2009; 93:21–23. [PubMed: 18621794]

Bromberg KD, Burgin AB, Osheroff N. Quinolone action against human topoisomerase IIalpha: stimulation of enzyme-mediated double-stranded DNA cleavage. Biochemistry. 2003; 42:3393–3398. [PubMed: 12653542]

Callegan MC, Ramirez R, Kane ST, Cochran DC, Jensen H. Antibacterial activity of the fourth-generation fluoroquinolones gatifloxacin and moxifloxacin against ocular pathogens. Adv Ther. 2003; 20:246–252. [PubMed: 14964344]

Chan HS, DeBoer G, Thiessen JJ, Budning A, Kingston JE, O'Brien JM, Koren G, Giesbrecht E, Haddad G, Verjee Z, Hungerford JL, Ling V, Gallie BL. Combining cyclosporin with chemotherapy controls intraocular retinoblastoma without requiring radiation. Clin Cancer Res. 1996; 2:1499–1508. [PubMed: 9816326]

Chan HS, Lu Y, Grogan TM, Haddad G, Hipfner DR, Cole SP, Deeley RG, Ling V, Gallie BL. Multidrug resistance protein (MRP) expression in retinoblastoma correlates with the rare failure of chemotherapy despite cyclosporine for reversal of P-glycoprotein. Cancer Res. 1997; 57:2325–2330. [PubMed: 9192801]

Chan HS, Thorner PS, Haddad G, Gallie BL. Multidrug-resistant phenotype in retinoblastoma correlates with P-glycoprotein expression. Ophthalmology. 1991; 98:1425–1431. [PubMed: 1682862]

Chen G, Teicher BA, Frei E 3rd. Differential interactions of Pgp inhibitor thaliblastine with adriamycin, etoposide, taxol and anthrapyrazole CI941 in sensitive and multidrug-resistant human MCF-7 breast cancer cells. Anticancer Res. 1996; 16:3499–3505. [PubMed: 9042212]

Chintagumpala M, Chevez-Barrios P, Paysse EA, Plon SE, Hurwitz R. Retinoblastoma: review of current management. Oncologist. 2007; 12:1237–1246. [PubMed: 17962617]

Dalhoff A, Shalit I. Immunomodulatory effects of quinolones. Lancet Infect Dis. 2003; 3:359–371. [PubMed: 12781508]

Dimaras H, Heon E, Doyle J, Strahlendorf C, Paton KE, Halliday W, Babyn P, Gallie BL, Chan HS. Multifaceted chemotherapy for trilateral retinoblastoma. Arch Ophthalmol. 129:362–365. [PubMed: 21402997]

Fabian I, Reuveni D, Levitov A, Halperin D, Priel E, Shalit I. Moxifloxacin enhances antiproliferative and apoptotic effects of etoposide but inhibits its proinflammatory effects in THP-1 and Jurkat cells. Br J Cancer. 2006; 95:1038–1046. [PubMed: 17047652]

Gokulgandhi MR, Barot M, Bagui M, Pal D, Mitra AK. Transporter-targeted lipid prodrugs of cyclic cidofovir: a potential approach for the treatment of cytomegalovirus retinitis. J Pharm Sci. 101:3249–3263. [PubMed: 22499243]

Gruss-Fischer T, Fabian I. Protection by ascorbic acid from denaturation and release of cytochrome c, alteration of mitochondrial membrane potential and activation of multiple caspases induced by H(2)O(2), in human leukemia cells. Biochem Pharmacol. 2002; 63:1325–1335. [PubMed: 11960609]

Hariharan S, Minocha M, Mishra GP, Pal D, Krishna R, Mitra AK. Interaction of ocular hypotensive agents (PGF2 alpha analogs-bimatoprost, latanoprost, and travoprost) with MDR efflux pumps on the rabbit cornea. J Ocul Pharmacol Ther. 2009; 25:487–498. [PubMed: 20028257]

Horowitz NS, Hua J, Gibb RK, Mutch DG, Herzog TJ. The role of topotecan for extending the platinum-free interval in recurrent ovarian cancer: an in vitro model. Gynecol Oncol. 2004; 94:67–73. [PubMed: 15262121]

Jain R, Agarwal S, Majumdar S, Zhu X, Pal D, Mitra AK. Evasion of P-gp mediated cellular efflux and permeability enhancement of HIV-protease inhibitor saquinavir by prodrug modification. Int J Pharm. 2005; 303:8–19. [PubMed: 16137847]

Kernt M, Neubauer AS, Liegl RG, Lackerbauer CA, Eibl KH, Alge CS, Ulbig MW, A AK. Intracameral moxifloxacin: in vitro safety on human ocular cells. Cornea. 2009; 28:553–561. [PubMed: 19421040]

Krishnakumar S, Mallikarjuna K, Desai N, Muthialu A, Venkatesan N, Sundaram A, Khetan V, Shanmugam MP. Multidrug resistant proteins: P-glycoprotein and lung resistance protein expression in retinoblastoma. Br J Ophthalmol. 2004; 88:1521–1526. [PubMed: 15548804]

Lee TW, Yang SW, Kim CM, Hong WS, Youn DH. Chemosensitization to adriamycin by cyclosporin A and verapamil in human retinoblastoma cell lines. J Korean Med Sci. 1993; 8:104–109. [PubMed: 8397925]

McGee DH, Holt WF, Kastner PR, Rice RL. Safety of moxifloxacin as shown in animal and in vitro studies. Surv Ophthalmol. 2005; 50(Suppl 1):S46–S54. [PubMed: 16257310]

Mizukami Y, Jo WS, Duerr EM, Gala M, Li J, Zhang X, Zimmer MA, Iliopoulos O, Zukerberg LR, Kohgo Y, Lynch MP, Rueda BR, Chung DC. Induction of interleukin-8 preserves the angiogenic response in HIF-1alpha-deficient colon cancer cells. Nat Med. 2005; 11:992–997. [PubMed: 16127434]

Pal D, Mitra AK. MDR-and CYP3A4-mediated drug-drug interactions. J Neuroimmune Pharmacol. 2006; 1:323–339. [PubMed: 18040809]

Rautio J, Humphreys JE, Webster LO, Balakrishnan A, Keogh JP, Kunta JR, Serabjit-Singh CJ, Polli JW. In vitro p-glycoprotein inhibition assays for assessment of clinical drug interaction potential of new drug candidates: a recommendation for probe substrates. Drug Metab Dispos. 2006; 34:786–792. [PubMed: 16455806]

Reuveni D, Halperin D, Fabian I, Tsarfaty G, Askenasy N, Shalit I. Moxifloxacin increases anti-tumor and anti-angiogenic activity of irinotecan in human xenograft tumors. Biochem Pharmacol. 79:1100–1107. [PubMed: 20025849]

Reuveni D, Halperin D, Shalit I, Priel E, Fabian I. Quinolones as enhancers of camptothecin-induced cytotoxic and anti-topoisomerase I effects. Biochem Pharmacol. 2008; 75:1272–1281. [PubMed: 18191106]

Saravolatz LD, Leggett J. Gatifloxacin, gemifloxacin, and moxifloxacin: the role of 3 newer fluoroquinolones. Clin Infect Dis. 2003; 37:1210–1215. [PubMed: 14557966]

Scoper SV. Review of third-and fourth-generation fluoroquinolones in ophthalmology: in-vitro and in-vivo efficacy. Adv Ther. 2008; 25:979–994. [PubMed: 18836691]

Shalit I, Horev-Azaria L, Fabian I, Blau H, Kariv N, Shechtman I, Alteraz H, Kletter Y. Immunomodulatory and protective effects of moxifloxacin against Candida albicans-induced bronchopneumonia in mice injected with cyclophosphamide. Antimicrob Agents Chemother. 2002; 46:2442–2449. [PubMed: 12121916]

Shalit I, Kletter Y, Halperin D, Waldman D, Vasserman E, Nagler A, Fabian I. Immunomodulatory effects of moxifloxacin in comparison to ciprofloxacin and G-CSF in a murine model of cyclophosphamide-induced leukopenia. Eur J Haematol. 2001; 66:287–296. [PubMed: 11422407]

Shields JA, Augsburger JJ. Current approaches to the diagnosis and management of retinoblastoma. Surv Ophthalmol. 1981; 25:347–372. [PubMed: 7017985]

Shields JA, Shields CL, Parsons HM. Differential diagnosis of retinoblastoma. Retina. 1991; 11:232–243. [PubMed: 1925090]

Vene R, Arena G, Poggi A, D'Arrigo C, Mormino M, Noonan DM, Albini A, Tosetti F. Novel cell death pathways induced by N-(4-hydroxyphenyl)retinamide: therapeutic implications. Mol Cancer Ther. 2007; 6:286–298. [PubMed: 17237288]

Wang Q, Strab R, Kardos P, Ferguson C, Li J, Owen A, Hidalgo IJ. Application and limitation of inhibitors in drug-transporter interactions studies. Int J Pharm. 2008; 356:12–18. [PubMed: 18272304]

Weiss T, Shalit I, Blau H, Werber S, Halperin D, Levitov A, Fabian I. Anti-inflammatory effects of moxifloxacin on activated human monocytic cells: inhibition of NF-kappaB and mitogen-activated protein kinase activation and of synthesis of proinflammatory cytokines. Antimicrob Agents Chemother. 2004; 48:1974–1982. [PubMed: 15155187]

Wilson MW, Fraga CH, Rodriguez-Galindo C, Hagedorn N, Leggas ML, Stewart C. Expression of the multi-drug resistance proteins and the pregnane X receptor in treated and untreated retinoblastoma. Curr Eye Res. 2009; 34:386–394. [PubMed: 19401882]

Wu WC, Hu DN, Gao HX, Chen M, Wang D, Rosen R, McCormick SA. Subtoxic levels hydrogen peroxide-induced production of interleukin-6 by retinal pigment epithelial cells. Mol Vis. 16:1864–1873. [PubMed: 21031020]

Highlights

- We examine moxifloxacin substrate specificity toward efflux transporters.
- We examine moxifloxacin interaction with chemotherapeutics for retinoblastoma.
- Moxifloxacin modulates permeability of anticancer agents at cellular efflux sites.
- Moxifloxacin also potentiate anticancer activity in retinoblastoma cells.

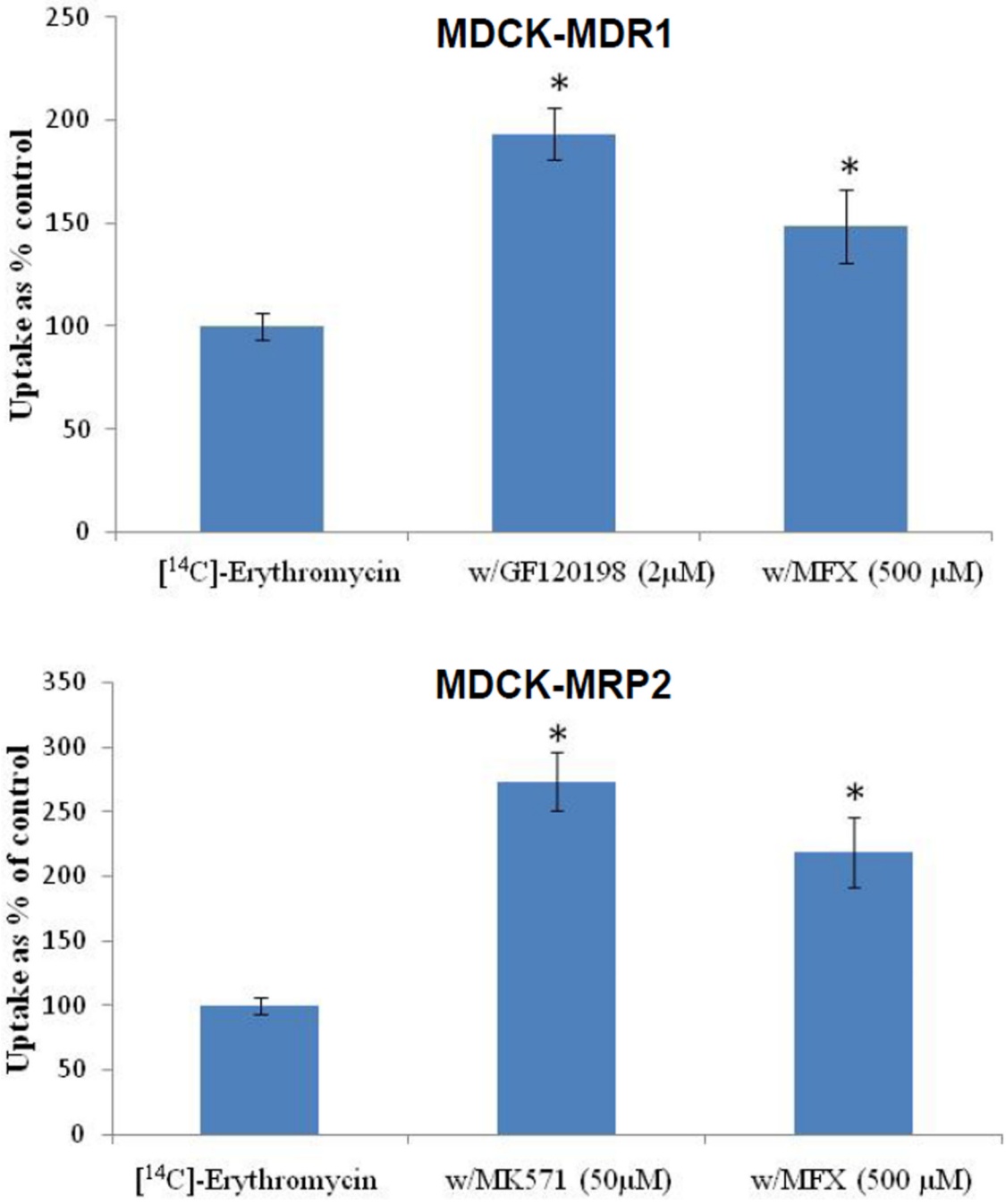

FIGURE 1.

Cellular accumulation of [^{14}C]-Erythromycin (0.25 μCi/mL) alone and in presence of moxifloxacin (500 μM), GF120198 (2 μM) and MK571 (50 μM) across MDCK-MDR1 and MDCK-MRP2 cells. Values are expressed as mean ± SD (n=4). *Data were considered statistically significant for $P \leq 0.05$.

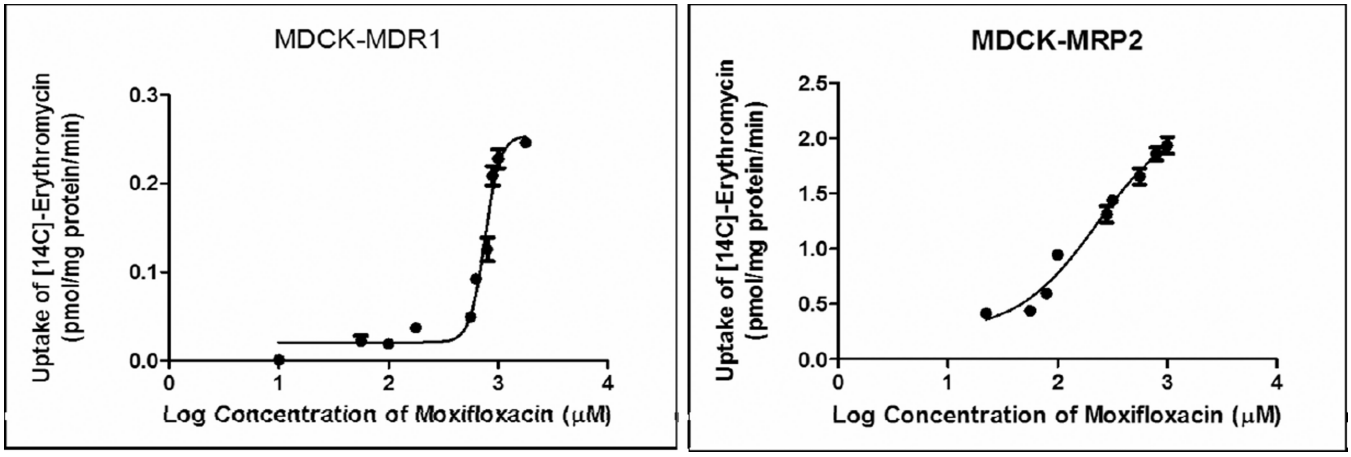

FIGURE 2.

Dose dependent moxifloxacin (10μM - 1mM) mediated inhibition of [^{14}C]-Erythromycin (0.25 μCi/mL) efflux across MDCK-MDR1 and MDCK-MRP2 cells. Values are expressed as mean ± SD (n=4).

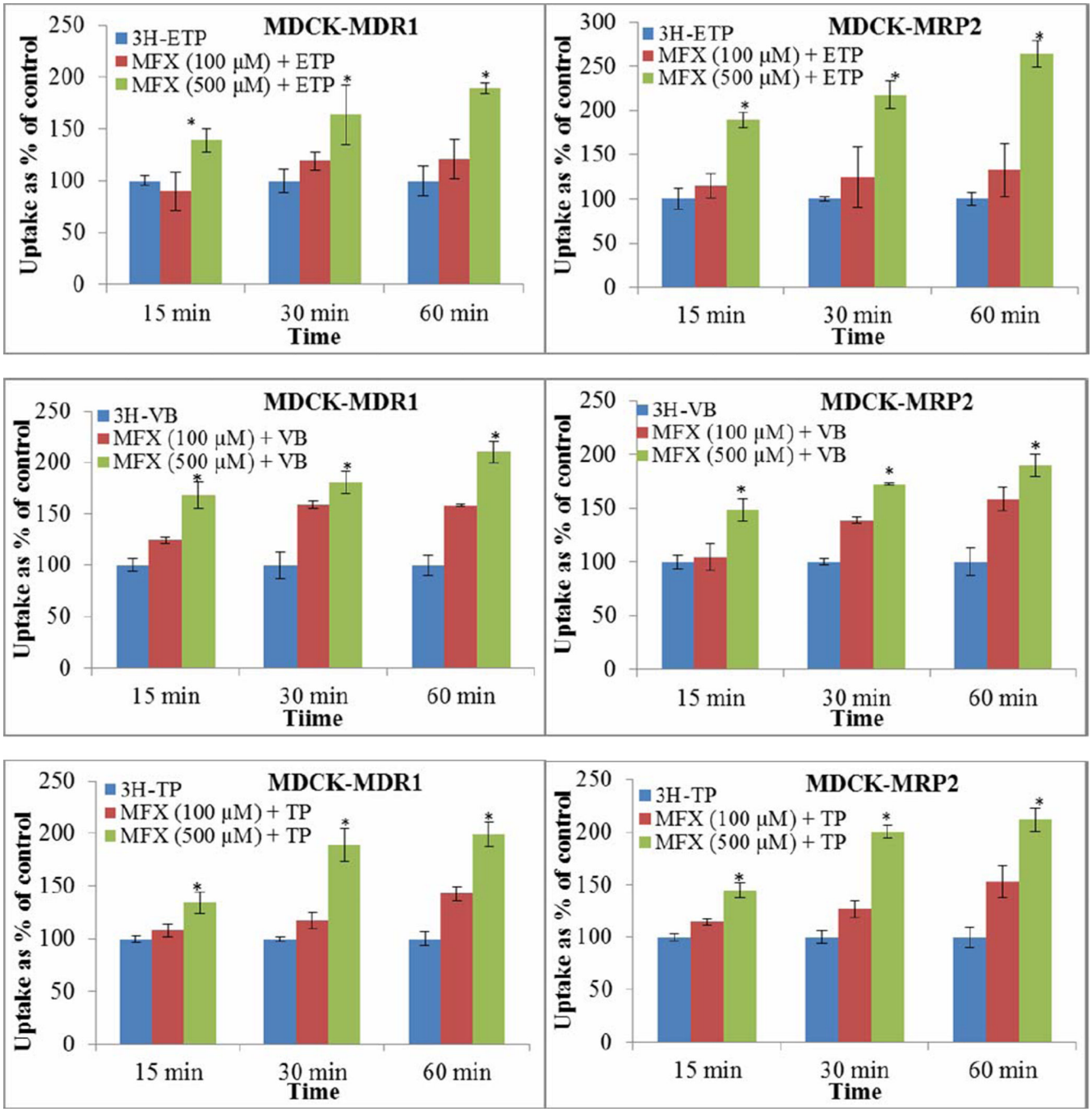

FIGURE 3.

Time and concentration dependent cellular accumulation of [^{3}H]-Etoposide, [^{3}H]-Topotecan and [^{3}H]-Vinblastine (each 0.25 μCi/mL) alone and in presence of moxifloxacin (100 and 500 μM) across MDCK-MDR1 and MDCK-MRP2 cells. Values are expressed as mean ± SD (n=4). *Data were considered statistically significant for $P \leq 0.05$. Moxifloxacin (MFX); Etoposide (ETP); Topotecan (TP); Vinblastine (VB).

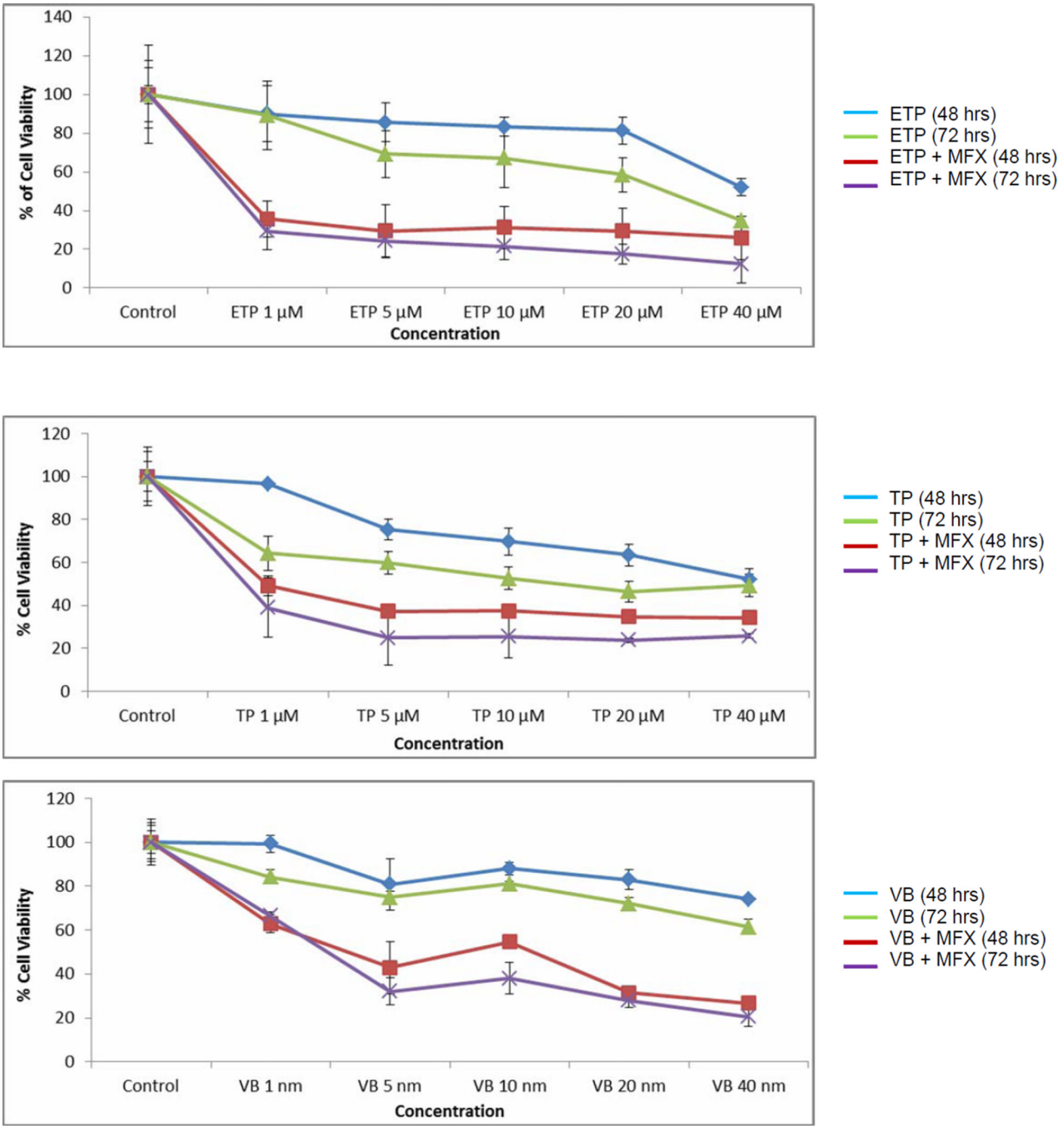

FIGURE 4.

Modulation of etoposide (1–40 µM), topotecan (1–40 µM), and vinblastine (1–40 nM) cytotoxicity on Y-79 cells by moxifloxacin (500 µM). Values are expressed as mean ± SD (n=6).

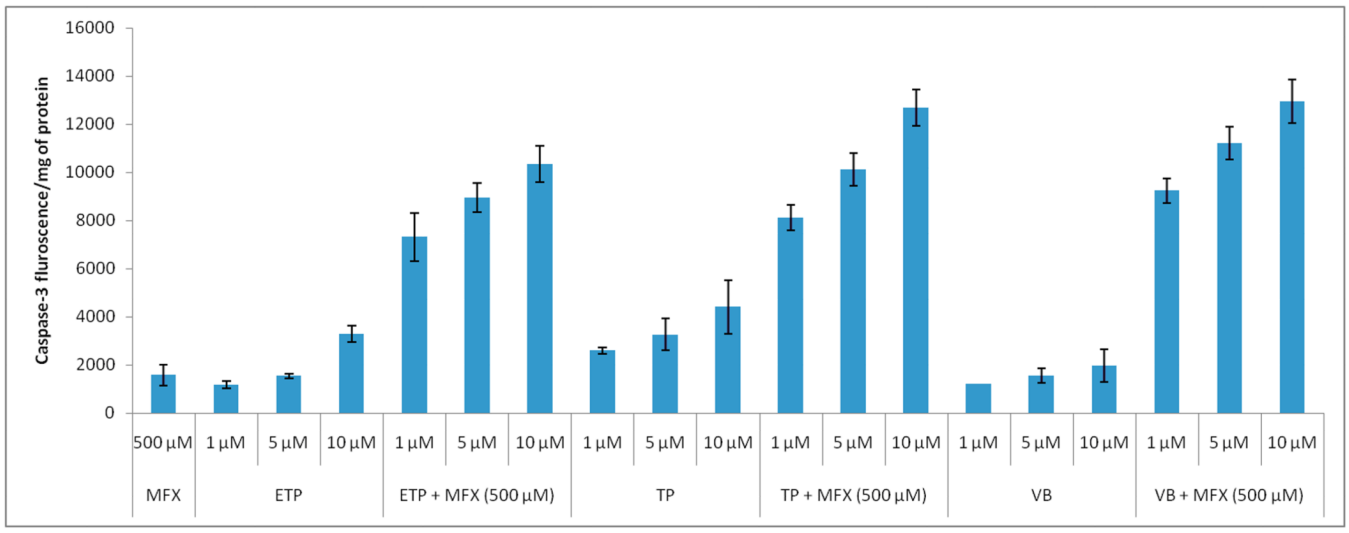

FIGURE 5.

Modulation of anticancer agents mediated caspase-3 activity on Y-79 cells by moxifloxacin. Values are expressed as mean ± SD (n=3). Moxifloxacin (MFX); Etoposide (ETP); Topotecan (TP); Vinblastine (VB).

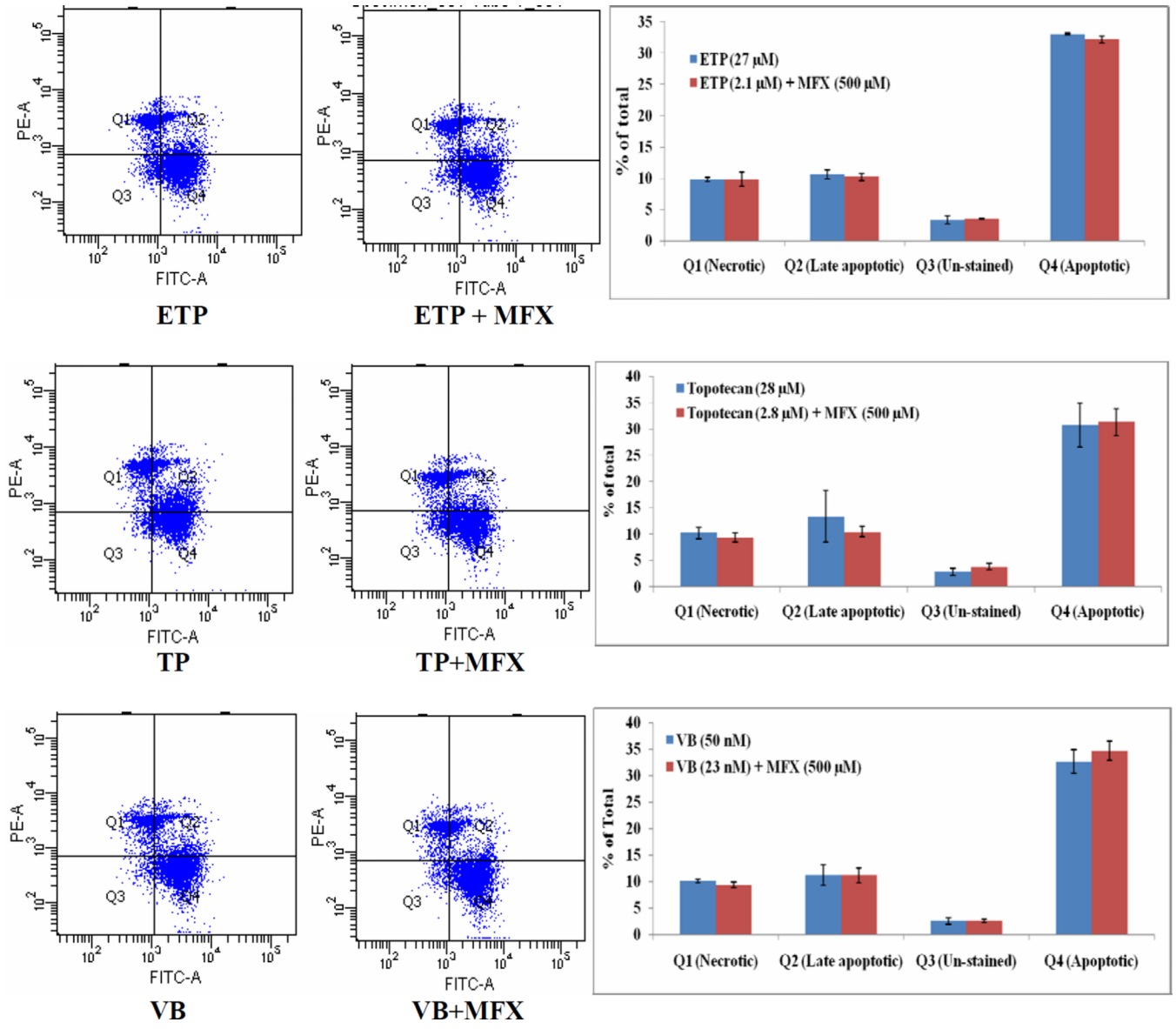

Figure 6.

Flow cytometry analysis using Annexin V (AV) and propidium iodide (PI) staining illustrating modulation of etoposide (ETP), topotecan (TP), and vinblastine (VB) mediated Y-79 cell apoptosis by moxifloxacin (MFX). Q1= PI positive cells ($AV^{-}PI^{+}$); Q2 = Late apoptotic (dead) cells ($AV^{+}PI^{+}$); Q3 = Un-stained (non-apoptotic healthy) cells ($AV^{-}PI^{-}$); Q4 = Early apoptotic (but viable) cells ($AV^{+}PI^{-}$).

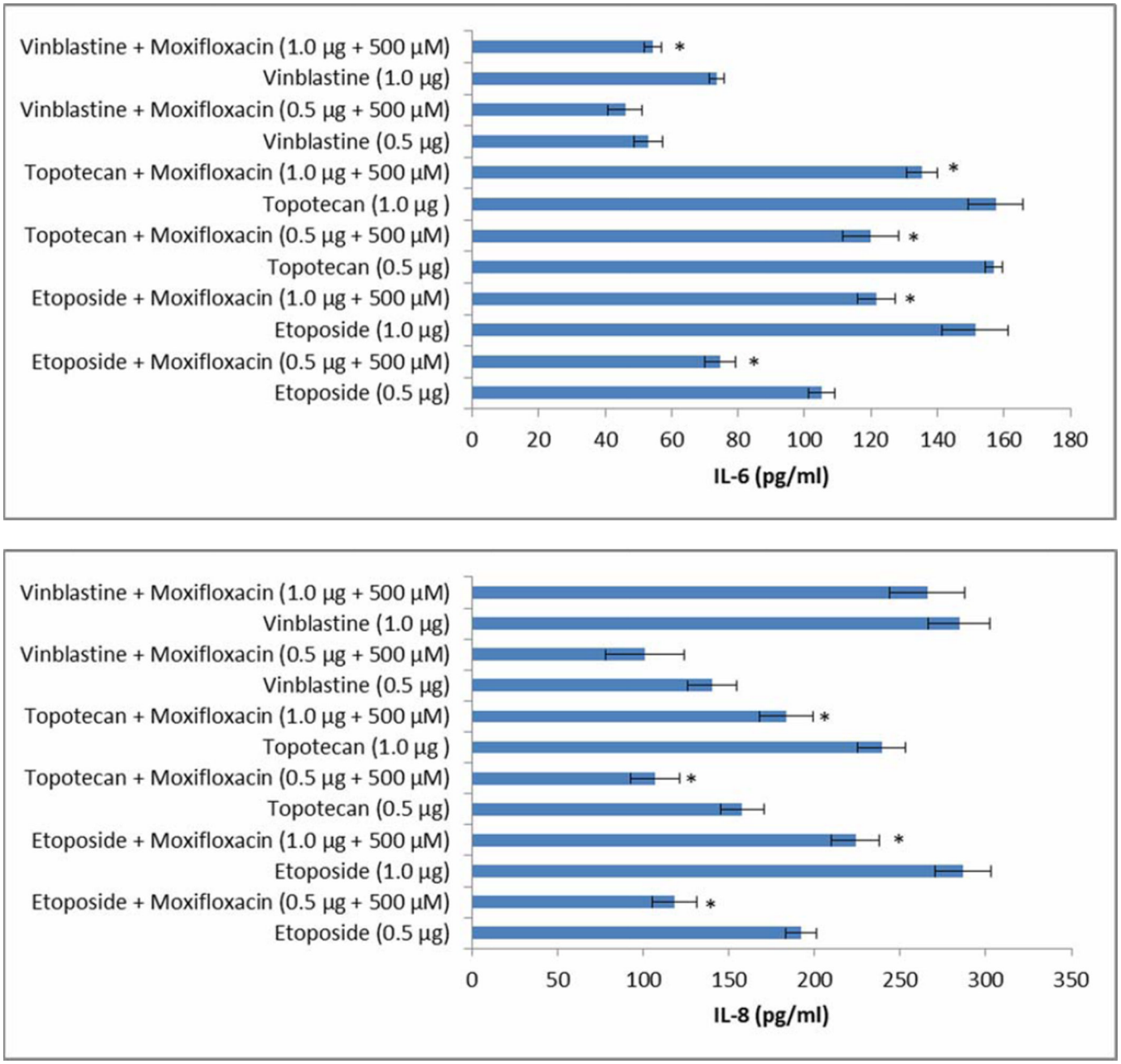

FIGURE 7.

Modulation of anticancer induced release of IL-6 and IL-8 by moxifloxacin across ARPE19 cells. Values are expressed as mean ± SD (n=4). Individual anticancer agents act as a control.

Table I

Bi-directional transport of moxifloxacin (500 μM) alone and in presence of GF120198 (2 μM) and MK571 (50 μM) across MDCK-MDR1, MDCK-MRP2 and MDCK-WT cells. Values are expressed as mean ± SD (n=4).

Cell line	Drug	Permeability (× 10^{-6})cm/s		Efflux Ratio
		AP-BL	BL-AP	
MDCK-MDR1	Moxifloxacin	5.81±0.44	20.46±2.26	3.52
	Moxifloxacin + GF120918	16.29±0.94	20.36±1.81	1.25
MDCK-MRP2	Moxifloxacin	0.78±0.13	1.97±0.41	2.53
	Moxifloxacin + MK571	1.64±0.17	1.86±0.24	1.20
MDCK-WT	Moxifloxacin	5.70 ± 0.04	7.40 ± 0.14	1.29
	Moxifloxacin + GF120918	6.62 ± 0.09	7.82 ± 0.07	1.18

Table II

Bi-directional transport of [^{3}H]-Etoposide, [^{3}H]-Topotecan and [^{3}H]-Vinblastine alone and in presence of moxifloxacin (500 μM), GF120198 (2 μM) and MK571 (50 μM) across MDCK-MDR and MDCK-MRP2. Values are expressed as mean ± SD (n=3).

Cell line	Drug	Permeability (×10^{-6}) cm/s		Efflux Ratio
		AP-BL	BL-AP	
MDCK-MDR1	Etoposide	3.57 ± 0.65	11.60 ± 1.78	3.25
	Etoposide + Moxifloxacin	7.92 ± 1.78	12.84 ± 2.08	1.62
	Etoposide + GF120918	10.71 ± 0.52	11.02 ± 1.45	1.03
	Vinblastine	1.55 ± 0.03	10.22 ± 0.47	6.59
	Vinblastine + Moxifloxacin	3.95 ± 0.46	8.92 ± 1.91	2.26
	Vinblastine + GF120918	5.35 ± 0.40	7.14 ± 1.47	1.33
	Topotecan	0.75 ± 0.03	3.50 ± 0.28	4.63
	Topotecan + Moxifloxacin	1.56 ± 0.03	3.38 ± 0.16	2.16
	Topotecan + GF120918	2.27 ± 0.18	3.14 ± 0.20	1.38
MDCK-MRP2	Etoposide	37.82 ± 2.70	206.76 ± 17.45	5.46
	Etoposide + Moxifloxacin	89.34 ± 1.75	194.29 ± 12.58	2.17
	Etoposide + MK571	175.62 ± 7.47	189.47 ± 20.42	1.08
	Vinblastine	13.50 ± 3.24	73.75 ± 8.16	5.46
	Vinblastine + Moxifloxacin	19.72 ±2.56	48.90 ± 6.70	2.48
	Vinblastine + MK571	25.60 ± 4.42	35.58± 9.72	1.39
	Topotecan	8.06 ± 0.66	24.78 ± 2.44	3.07
	Topotecan + Moxifloxacin	12.67 ± 2.67	22.89 ± 3.54	1.80
	Topotecan + MK571	19.51 ± 1.31	22.08 ± 2.79	1.13